

# Study of the transverse momentum distribution of transport models of kaon, Pion, and (anti-)proton production in U+U collisions at $\sqrt{s_{NN}} = 193$ GeV

Ying Yuan,<sup>1,2\*</sup>

1) *College of Pharmacy,  
Guangxi University of Chinese Medicine,  
Nanning 530200, China*

2) *Guangxi Key Laboratory of Nuclear Physics and Nuclear Technology,  
Guangxi Normal University,  
Guilin 541004, China*

## Abstract

In this study, the transverse momentum spectra of  $k^\pm$ ,  $\pi^\pm$  and  $p(\bar{p})$  particles in mid-rapidity ( $|y| < 0.1$ ) for nine centrality classes are investigated in  $^{238}\text{U}+^{238}\text{U}$  collisions at  $\sqrt{s_{NN}}=193$  GeV within the cascade and soft momentum-dependent equation of state (SM-EoS) mode of the UrQMD model. Other extracted observable from  $p_T$  spectrum includes average transverse momentum ( $\langle p_T \rangle$ ), the yield ( $dN/dy$ ) as well as the ratio of particle type are also shown in function of collision centrality. It is found that the U+U collision process is subregional with considering the deformation of Uranium nucleus. The experimental data are described well using cascade mode when the  $p_T < 1.2\text{GeV}/c$ . The theoretical calculation results using the SM-EoS mode are basically consistent with the trend of the experimental data at  $p_T > 1.2\text{GeV}/c$ . At RHIC energy, it is also found that pair production is the dominant production mechanism for particles, with the anti-ion to ion yield ratio suggesting.

PACS numbers: 24.10.Lx, 25.75.Dw, 25.75.-q

Keywords: UrQMD model; cascade; SM-EoS; transverse momentum distributions; U+U collisions

---

\* E-mail address: yuany@gxtnmu.edu.cn

## I. INTRODUCTION

Heavy-ion collisions (HICs) at ultra-relativistic energies present a unique opportunity to study properties of strongly interacting matter at extreme temperatures and densities<sup>[1–7]</sup>. Understanding the mechanisms of particles and fragment generation in super-relativistic HICs is important because it may provide information about the phase transition of quantum chromodynamics (QCD) from quark- gluon plasma (QGP) to hadron gas (HG)<sup>[8, 9]</sup>. Over the past two decades, many experiments have been conducted at the Relativistic Heavy Ion Collider (RHIC) near the critical energy of the hadronic matter to QGP phase transition.<sup>[10]</sup> Theoretical studies on particle and antiparticle generation have been carried out for many years, such as statistical model, coalescence model and transport model<sup>[11–19]</sup>. The investigation of transport phenomena is particularly crucial in comprehending numerous fundamental properties<sup>[20]</sup>. One of the reasons to study transverse momentum spectra of particles produced in high-energy collisions is their ability to provide critical information about the frozen state of the dynamics of interacting systems<sup>[21]</sup>. At the Relativistic Heavy Ion Collider (RHIC), experiments have demonstrated that in U+U collisions with a center of mass energy of 193 GeV, a highly dense system of defined quarks and gluons forms, creating a very hot and dense medium<sup>[22]</sup>.

The ultra-relativistic quantum molecular dynamics (UrQMD) method is utilized to generate the transverse momentum distributions of  $\pi$  mesons, kaons, and  $p(\bar{p})$  particles in U+U collisions at a center-of-mass energy of 193 GeV. The study also considers the presence of collisional interactions between particles. Comparisons are made with experimental data collected by the STAR Collaboration<sup>[23]</sup>. The primary objective of this research is to obtain information about the behavior of nuclear reactions that could be used to understand the final state particle production in U+U collisions at the RHIC energy.

## II. ULTRARELATIVISTIC QUANTUM MOLECULAR DYNAMICS TRANSPORT MODEL

### A. The ultra-relativistic quantum molecular dynamics (UrQMD) model

The UrQMD model is a microscopic many-body approach to transport that can be applied to study the interactions of protons with protons (pp), with protons on a nucleus (pA)

with a nucleus on a nucleus (AA) over the energy range from the Spheron Ion Source to the Large Hadron Collider. This model is based on the propagation of color strings, of which the constituent quarks and diquarks (as the end of the string) carry mesonic and baryonic degrees of freedom<sup>[24]</sup>. It can combine different reaction mechanisms and provide theoretical simulations of various experimental observations. Currently, in our model, subhadrons' degrees of freedom enter through a formation time for hadrons resulting from string fragmentation, which is dominant at the early stages of heavy-ion collisions (HICs) at high SPS and RHIC energies<sup>[25–27]</sup>.

Like the quantum molecular dynamics (QMD) model, the UrQMD model follows parallel principles to simulate hadrons in phase space with the propagation of each individual hadron's phase space according to Hamilton's equation of motion<sup>[28]</sup>,

$$\dot{\vec{r}}_i = \frac{\partial H}{\partial \vec{p}_i}, \quad \dot{\vec{p}}_i = -\frac{\partial H}{\partial \vec{r}_i}. \quad (1)$$

Here,  $\vec{r}_i$  and  $\vec{p}_i$  are the coordinate and momentum of the hadron  $i$ , and the Hamiltonian  $H$  consists of the kinetic energy  $T$  and the effective interaction potential energy  $U$ ,

$$H = T + U. \quad (2)$$

This microscopic transport approach simulates the interactions of incoming and newly produced particles, the excitation and fragmentation of color strings and the formation and decay of hadronic resonances. In the pursuit of higher energies, it is crucial to consider the treatment of subhadronic degrees of freedom. In this current version, the degrees of freedom are introduced through a hadron formation time, in the string fragmentation process, and there is no explicit incorporation of a phase transition from a hadronic to a quark-gluon phase in the model's dynamics. However, a detailed analysis of the model in thermal equilibrium yields an effective equation of state of the Hagedorn type<sup>[29]</sup>.

For the initialization part, the nucleon density distribution in the ground state follows the Woods Saxon distribution,

$$\rho(r, \theta, \phi) = \frac{\rho_0}{1 + e^{[(r-R(\theta, \phi))/a]}} \quad (3)$$

Here,  $\rho_0=0.16 \text{ fm}^{-3}$ ,  $a = 0.55 \text{ fm}$ . Considering the quadrupole deformation of uranium nuclei<sup>[30]</sup>,

$$R(\theta, \phi) = R_0[1 + \beta_2 Y_{20}(\theta, \phi)] \quad (4)$$

and  $R_0 = 1.16A^{\frac{1}{3}}$ ,  $\beta_2 = 0.28$  <sup>[31, 32]</sup>. In the calculation of this paper, we simulate the results of the random orientation collision between the projectile and the target core.

### B. The soft momentum dependent equation of state (SM-EoS)

In the standard framework of the UrQMD model, the term "potential energy" incorporates various types of interactions such as those involving the two-body and three-body Skyrme-, Yukawa-, Coulomb- and Pauli-terms <sup>[16, 28, 33]</sup>,

$$U = U_{\text{sky}}^{(2)} + U_{\text{sky}}^{(3)} + U_{\text{Yuk}} + U_{\text{Cou}} + U_{\text{pau}}. \quad (5)$$

In the upgraded UrQMD (version 3.4) of the present work, additional terms are defined: (1) the density-dependent symmetry potential term  $U_{\text{sym}}$  and (2) the momentum-dependent term  $U_{\text{md}}$  <sup>[34]</sup>. In this study, the soft momentum-dependent (SM) equation of state (EoS) is applied, which is presented in Ref. [35]. In the RHIC energy regime, the Yukawa-, Pauli-, and baryon symmetry potentials become unimportant, while the Skyrme and momentum-dependence parts of potentials still affect the full HIC dynamic process <sup>[36]</sup>. During the formation time, the "pre-formed" particles (string fragments that will be abducted onto hadronic states later on) are usually treated to be free streaming, while reduced cross sections are only included for leading hadrons.

In this paper, the transverse momentum distributions and central yields of  $\pi$  mesons,  $k$  mesons and  $p(\bar{p})$  generated in U+U collisions at  $\sqrt{s_{NN}}=193$  GeV at mid-rapidity ( $|y|<0.1$ ) are studied by using UrQMD cascade mode and SM-EoS mode.

## III. RESULTS AND DISCUSSIONS

### A. Transverse momentum spectrum

Fig. 1 is shown the transverse momentum spectra in nine centrality classes in U+U collisions at  $\sqrt{s_{NN}}=193$  GeV at mid-rapidity ( $|y|<0.1$ ) for  $\pi^+$  and  $\pi^-$ . There are nine centrality classes, representing a range of 0 – 5%, 5 – 10%, 10 – 20%, 20 – 30%, 30 – 40%, 40 – 50%, 50 – 60%, 60 – 70% and 70 – 80% respectively. The dotted lines are the results calculated from the cascade mode of UrQMD model. The solid lines are the results calculated from the soft momentum dependent equation of state mode of UrQMD model. The symbols are the experimental data from the STAR Collaboration <sup>[23]</sup>. The calculations are shown for

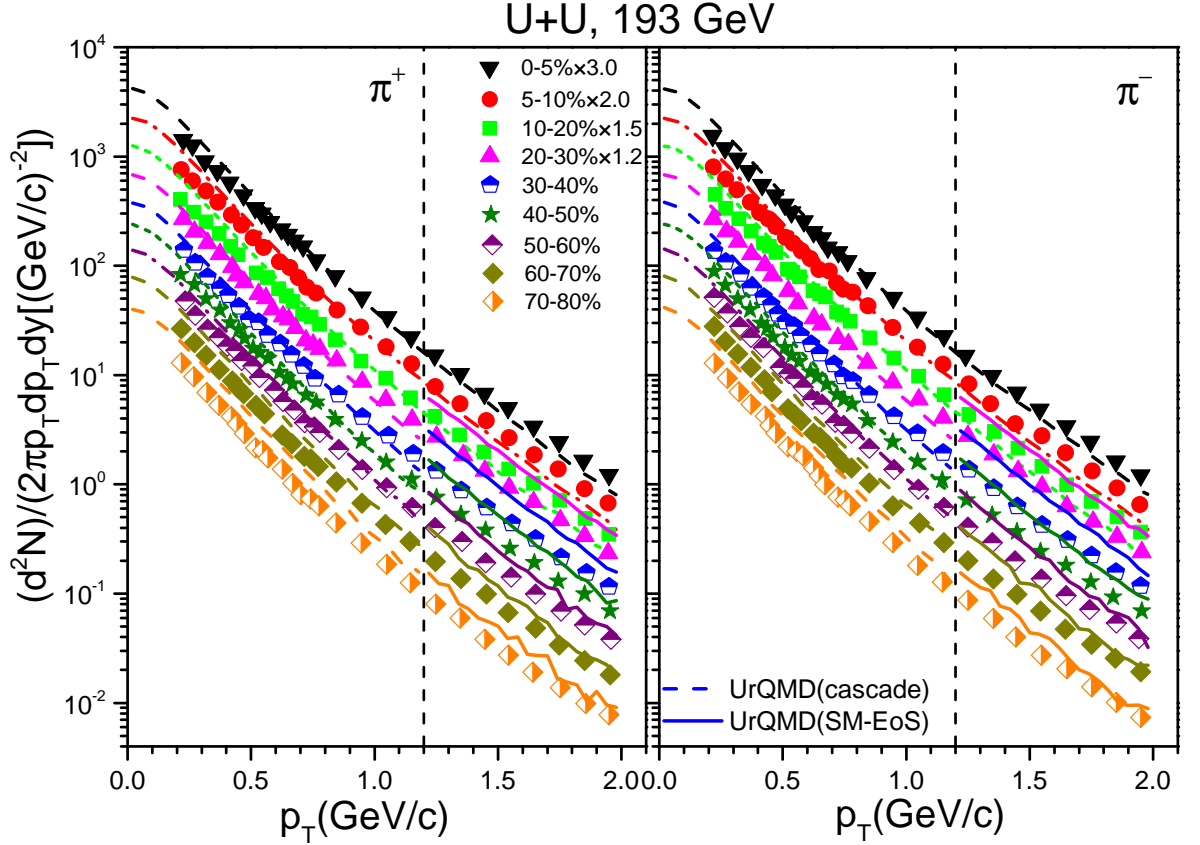


FIG. 1: Transverse momentum spectra of  $\pi^+$  and  $\pi^-$  are calculated at mid-rapidity ( $|y| < 0.1$ ) in U+U collisions at  $\sqrt{s_{NN}}=193$  GeV for 0 – 5%, 5 – 10%, 10 – 20%, 20 – 30%, 30 – 40%, 40 – 50%, 50 – 60%, 60 – 70% and 70 – 80% centralities from the cascade mode and the soft momentum dependent equation of state mode of UrQMD model. The lines denote calculations, while the symbol represents experimental data taken from the STAR Collaboration <sup>[23]</sup>.

$p_T < 2.0 \text{ GeV}/c$  in the Figure. The cascading mode of the UrQMD model has been observed to demonstrate significant agreement with empirical laws at centralities of 20 – 80% for  $p_T < 1.2 \text{ GeV}/c$  and at 0 – 20% centrality. However, in the transverse momentum region at 20 – 80% with  $1.2 \text{ GeV}/c < p_T < 2.0 \text{ GeV}/c$ , the theoretical yield of the SM-EoS model exceeds the experimental measurements. However, the higher the momentum is, the closer the theoretical description is to the experimental value. Due to the limitations of the UrQMD model in the physical description of some partons, it overestimates the yield of  $\pi$  mesons in

the medium transverse momentum region.

Fig. 2 is shown the transverse momentum spectra in nine centrality classes in U+U collisions at  $\sqrt{s_{NN}}=193$  GeV at mid-rapidity ( $|y|<0.1$ ) for  $k^+$  and  $k^-$ . The dotted lines are the results calculated from the cascade mode of UrQMD model. The solid lines are the results calculated from the soft momentum dependent equation of state mode of UrQMD model. The symbols are the experimental data from the STAR Collaboration <sup>[23]</sup>. The calculations for transverse momentum ( $p_T$ ) below 2.0 GeV/c are presented in the figure. The cascading mode of the UrQMD model has been found to exhibit significant agreement with empirical laws for  $p_T < 1.2$  GeV/c. However, it is observed that as the transverse momentum decreases, the theoretical values tend to be overestimated. Furthermore, with an increase in collision centrality, the range of overestimation in transverse momentum also expands. In the region where  $1.2\text{GeV}/c < p_T < 2.0\text{GeV}/c$  at centralities ranging from 20% to 80%, the theoretical predictions align closely with experimental results. Conversely, at a centrality of 0 – 20%, the theoretical yield predicted by the SM-EoS model surpasses experimental measurements. This difference can be attributed to the fact that the UrQMD model cannot directly explain the phase transition effect in the quark-gluon plasma (QGP). Furthermore, the influence of the quark recombination mechanism on the yield of  $k$  mesons has not been considered either. Consequently, within central collision regions, there is an overestimation of transverse momentum distributions for  $k$  mesons.

Fig. 3 presents the transverse momentum spectra across nine centrality classes in U+U collisions at  $\sqrt{s_{NN}}=193$  GeV, measured at mid-rapidity ( $|y|<0.1$ ) for protons ( $p$ ) and antiprotons ( $\bar{p}$ ). The dotted lines represent results calculated using the cascade mode of the UrQMD model, while the solid lines correspond to outcomes derived from a soft momentum-dependent equation of state within the same model. The symbols denote experimental data obtained from the STAR Collaboration <sup>[23]</sup>. The calculations are displayed for  $p_T < 2.0\text{GeV}/c$  in this figure. It is evident from the figure that for protons for  $p_T < 2.0\text{GeV}/c$  and antiprotons for  $p_T > 1.2\text{GeV}/c$ , the theoretical predictions of transverse momentum distributions align well with experimental observations. However, in the region where  $p_T < 1.2\text{GeV}/c$ , there is a noticeable underestimation of theoretical values for antiprotons as collision centrality decreases. This discrepancy arises because the UrQMD model does not account for quark-gluon plasma phase transitions, which may lead to an underprediction of antiproton

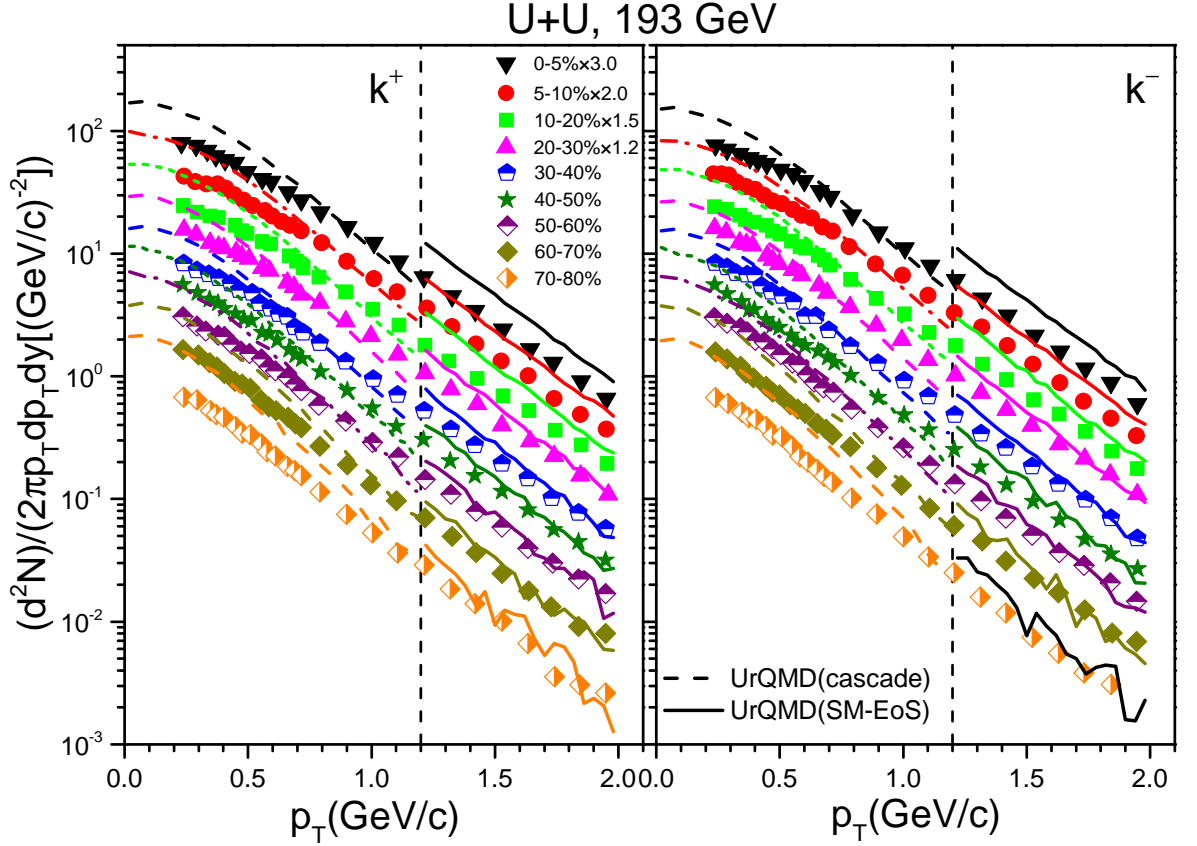


FIG. 2: Transverse momentum spectra of  $k^+$  and  $k^-$  are calculated at mid-rapidity ( $|y| < 0.1$ ) in U+U collisions at  $\sqrt{s_{NN}}=193$  GeV for 0 – 5%, 5 – 10%, 10 – 20%, 20 – 30%, 30 – 40%, 40 – 50%, 50 – 60%, 60 – 70% and 70 – 80% centralities from the cascade mode and the soft momentum dependent equation of state mode of UrQMD model. The lines denote calculations, while the symbol represents experimental data taken from the STAR Collaboration<sup>[23]</sup>.

yields in high-temperature and high-density environments.

In general, in the area of  $p_T < 1.2\text{GeV}/c$ , the cascade mode provides a more accurate description of the experimental results. In the  $1.2\text{GeV}/c < p_T < 2.0\text{GeV}/c$  region, however, the SM-EoS model offers a better fit to the data. Herein, we analyze the U+U collision process in a systematic manner by dividing it into distinct regions. Uranium nuclei are ellipsoidal in shape. In our calculations, we take into account their quadrupole deformation characteristics and assume that the collision probabilities for sharp-tip, body-body, and body-tip interactions are equivalent. As illustrated in Figures 1-3, during the initial stage of collision, there is a relatively high energy density in the central region. The particles

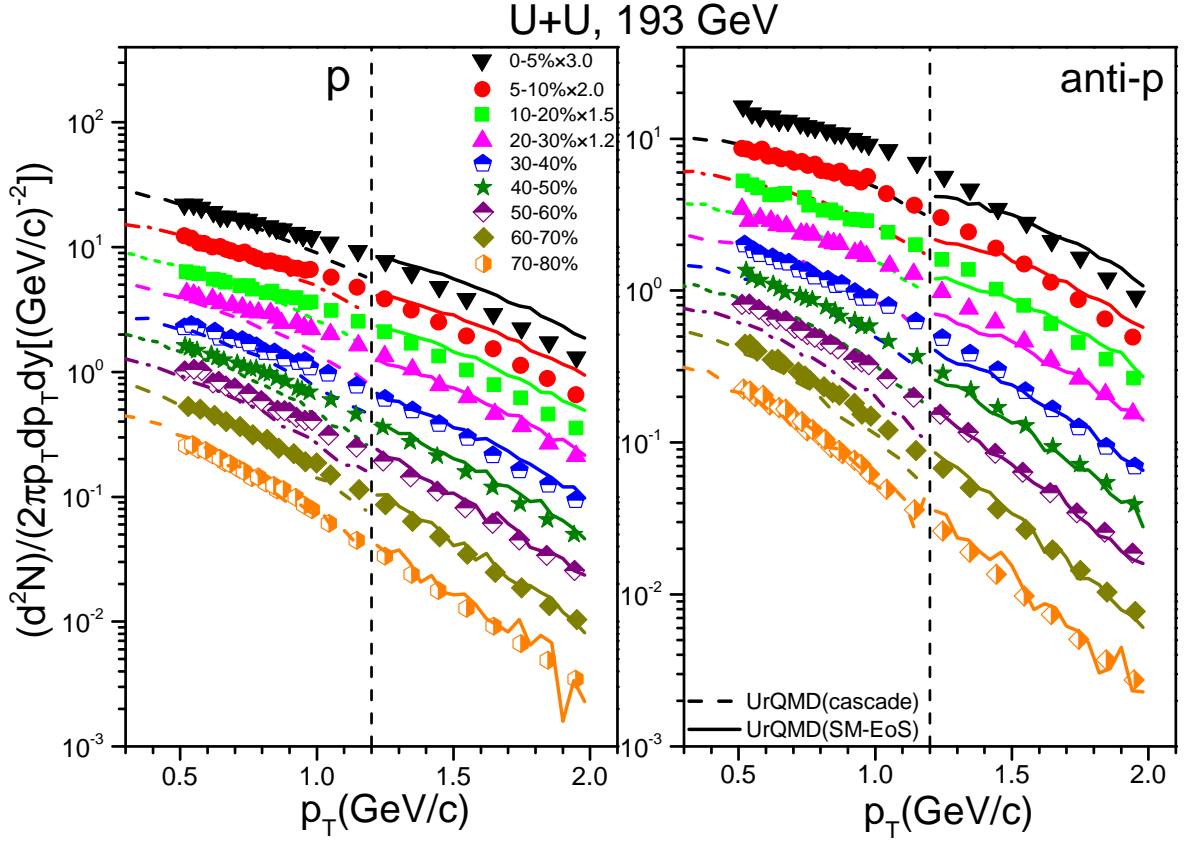


FIG. 3: Transverse momentum spectra of  $p$  and  $\bar{p}$  are calculated at mid-rapidity ( $|y| < 0.1$ ) in U+U collisions at  $\sqrt{s_{NN}}=193$  GeV for 0 – 5%, 5 – 10%, 10 – 20%, 20 – 30%, 30 – 40%, 40 – 50%, 50 – 60%, 60 – 70% and 70 – 80% centralities from the cascade mode and the soft momentum dependent equation of state mode of UrQMD model. The lines denote calculations, while the symbol represents experimental data taken from the STAR Collaboration<sup>[23]</sup>.

generated at this stage cannot rapidly escape from this central area; instead, they deposit part or all of their energy back into it. Consequently, at this point in time, the influence of the equation of state is minimal. As time progresses, previously produced particles begin to interact with other nucleons and gradually move away from the central region; thus, as these dynamics unfold, the impact of an average field becomes increasingly significant.

### B. Average transverse momentum distributions

Figure 4 shows the variation of  $\langle p_T \rangle$  with  $\langle N_{part} \rangle$  at midrapidity ( $|y| < 0.1$ ) for  $\pi^+$ ,  $k^+$  and  $p$  particles in U+U collisions at  $\sqrt{s_{NN}}=193$  GeV. The black diamonds were obtained from



UrQMD calculations, and the red solid circles are the experimental data <sup>[23]</sup>. It is found that the experimental results can be described within the tolerance of error. The values of  $\langle p_T \rangle$  increase slowly with the decrease of collision centrality, and they are listed in Table I.

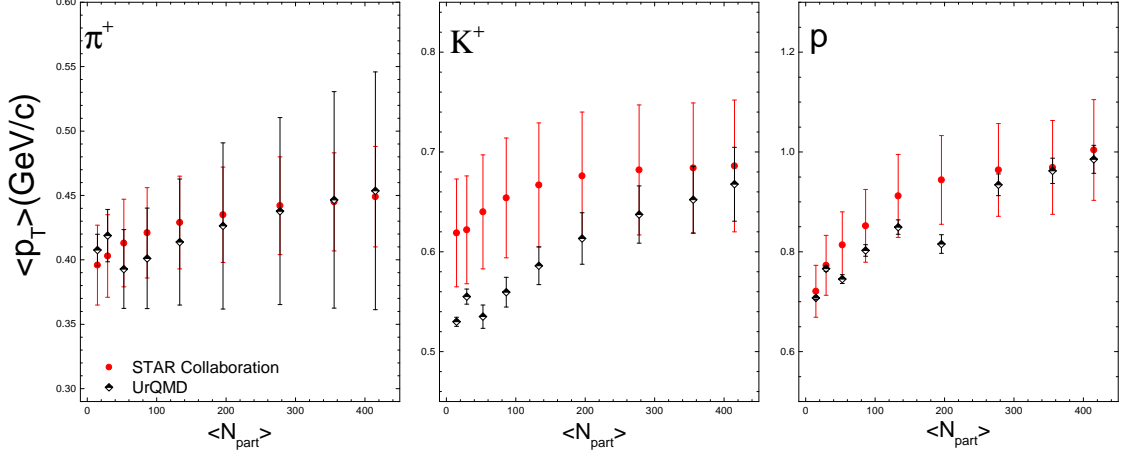


FIG. 4:  $\langle p_T \rangle$  as a function of  $\langle N_{part} \rangle$  at mid-rapidity ( $|y| < 0.1$ ) of  $\pi^+$ ,  $k^+$  and  $p$  for U+U collisions at  $\sqrt{s_{NN}}=193$  GeV. The red solid circles represent data collected by the STAR Collaboration <sup>[23]</sup>. The black diamonds are the calculation using UrQMD model.

### C. Particle yields

Fig. 5 shows  $dN/dy$  as a function of  $\langle N_{part} \rangle$  at mid-rapidity ( $|y| < 0.1$ ) for  $\pi^+$ ,  $K^+$ ,  $p$ , and  $\bar{p}$  in U+U collisions at  $\sqrt{s_{NN}} = 193$  GeV. The black diamonds represent the results calculated from the UrQMD model, while the red solid circles correspond to the experimental data <sup>[23]</sup>. The values of  $dN/dy$  increase gradually with decreasing collision centrality and are summarized in Table II. It is evident that the theoretical predictions for  $K^+$ ,  $p$ , and  $\bar{p}$  agree well with the experimental data within the allowable error range. However, the  $\pi^+$  mesons in peripheral collisions deviate significantly from the experimental results. This discrepancy arises because  $\pi$  mesons are predominantly produced via nucleon-nucleon interactions, nucleon resonance decays, and baryon intermediate states. Both nucleon resonance states and baryon intermediate states significantly influence the yield of  $\pi$  mesons. In peripheral colli-

TABLE I: Values of  $\langle p_T \rangle$  in GeV/c within mid-rapidity ( $|y| < 0.1$ ) of  $\pi^+$ ,  $\pi^-$ ,  $k^+$ ,  $k^-$ ,  $p$  and  $\bar{p}$  for U+U collisions at  $\sqrt{s_{NN}}=193$  GeV using the UrQMD model.

Centrality	$\pi^+$	$\pi^-$	$k^+$	$k^-$	$p$	$\bar{p}$
0-5%	$0.450 \pm 0.092$	$0.450 \pm 0.092$	$0.661 \pm 0.037$	$0.661 \pm 0.035$	$0.980 \pm 0.028$	$1.053 \pm 0.019$
5-10%	$0.445 \pm 0.082$	$0.445 \pm 0.082$	$0.651 \pm 0.033$	$0.649 \pm 0.031$	$0.960 \pm 0.025$	$1.028 \pm 0.017$
10-20%	$0.440 \pm 0.070$	$0.440 \pm 0.070$	$0.638 \pm 0.028$	$0.634 \pm 0.026$	$0.932 \pm 0.021$	$1.003 \pm 0.015$
20-30%	$0.432 \pm 0.057$	$0.432 \pm 0.057$	$0.620 \pm 0.022$	$0.616 \pm 0.021$	$0.915 \pm 0.017$	$0.961 \pm 0.013$
30-40%	$0.423 \pm 0.045$	$0.424 \pm 0.045$	$0.599 \pm 0.018$	$0.596 \pm 0.017$	$0.885 \pm 0.014$	$0.919 \pm 0.011$
40-50%	$0.415 \pm 0.036$	$0.415 \pm 0.036$	$0.580 \pm 0.014$	$0.574 \pm 0.013$	$0.844 \pm 0.011$	$0.874 \pm 0.009$
50-60%	$0.408 \pm 0.027$	$0.409 \pm 0.027$	$0.563 \pm 0.010$	$0.558 \pm 0.010$	$0.803 \pm 0.008$	$0.820 \pm 0.007$
60-70%	$0.388 \pm 0.026$	$0.389 \pm 0.026$	$0.522 \pm 0.010$	$0.518 \pm 0.009$	$0.750 \pm 0.006$	$0.880 \pm 0.006$
70-80%	$0.397 \pm 0.014$	$0.400 \pm 0.014$	$0.519 \pm 0.005$	$0.519 \pm 0.005$	$0.695 \pm 0.004$	$0.715 \pm 0.004$

TABLE II: Values of  $dN/dy$  within mid-rapidity ( $|y| < 0.1$ ) of  $\pi^+$ ,  $\pi^-$ ,  $k^+$ ,  $k^-$ ,  $p$  and  $\bar{p}$  for U+U collisions at  $\sqrt{s_{NN}}=193$  GeV using the UrQMD model.

Centrality	$\pi^+$	$\pi^-$	$k^+$	$k^-$	$p$	$\bar{p}$
0-5%	$485.32 \pm 1.12$	$518.46 \pm 1.44$	$69.52 \pm 0.56$	$62.19 \pm 0.53$	$36.74 \pm 0.44$	$18.24 \pm 0.31$
5-10%	$394.67 \pm 1.01$	$420.04 \pm 1.29$	$55.63 \pm 0.50$	$49.54 \pm 0.47$	$29.22 \pm 0.39$	$14.93 \pm 0.28$
10-20%	$287.96 \pm 0.87$	$305.06 \pm 1.10$	$40.43 \pm 0.43$	$36.35 \pm 0.40$	$21.19 \pm 0.33$	$11.29 \pm 0.24$
20-30%	$202.19 \pm 0.89$	$203.84 \pm 0.89$	$26.49 \pm 0.34$	$23.91 \pm 0.33$	$13.98 \pm 0.27$	$7.87 \pm 0.20$
30-40%	$131.33 \pm 0.71$	$132.93 \pm 0.71$	$16.85 \pm 0.27$	$15.37 \pm 0.26$	$9.04 \pm 0.21$	$5.37 \pm 0.17$
40-50%	$81.76 \pm 0.55$	$82.39 \pm 0.56$	$10.35 \pm 0.21$	$9.45 \pm 0.20$	$5.53 \pm 0.17$	$3.52 \pm 0.13$
50-60%	$47.79 \pm 0.42$	$48.29 \pm 0.42$	$6.00 \pm 0.16$	$5.49 \pm 0.15$	$3.24 \pm 0.13$	$2.18 \pm 0.10$
60-70%	$26.91 \pm 0.31$	$27.20 \pm 0.31$	$3.34 \pm 0.12$	$3.09 \pm 0.11$	$1.78 \pm 0.09$	$1.28 \pm 0.08$
70-80%	$13.76 \pm 0.22$	$13.87 \pm 0.22$	$1.70 \pm 0.08$	$1.58 \pm 0.08$	$0.89 \pm 0.06$	$0.67 \pm 0.05$

sions, the mean-field effect is considered, which slows down the escape of  $\pi$  mesons from the collision zone, thereby enhancing their production in this region. Additionally, insufficient consideration of initial fluctuations in the model may contribute to this deviation. These

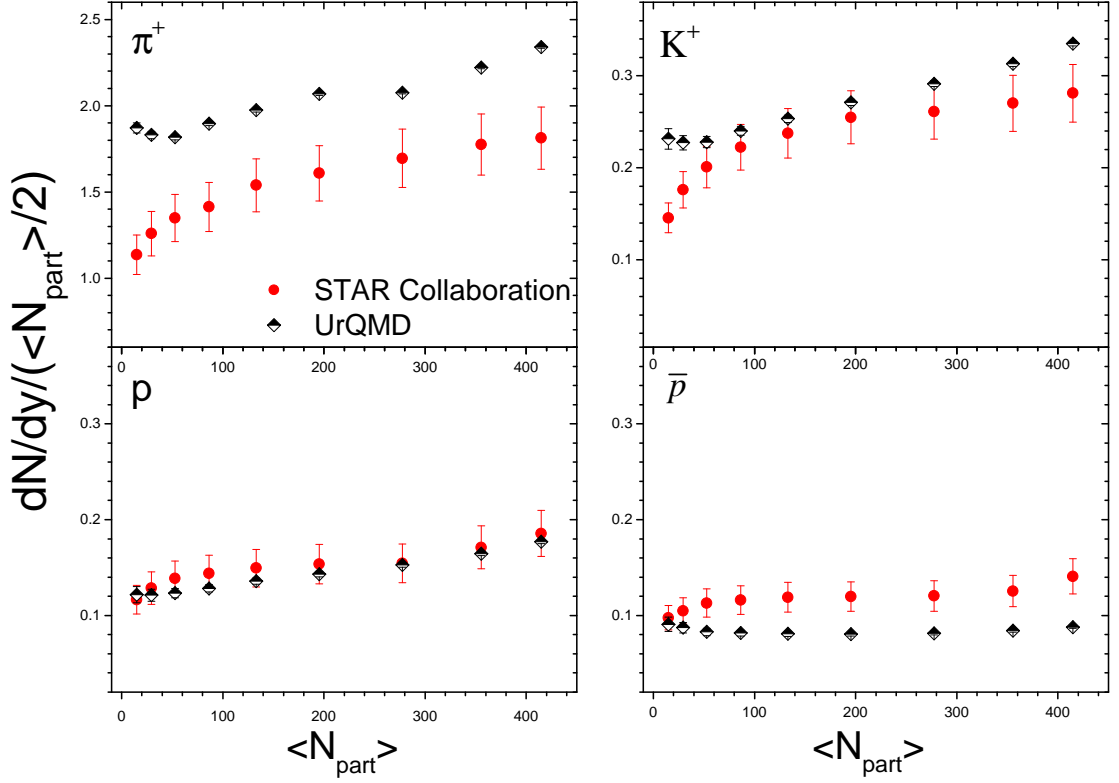


FIG. 5:  $dN/dy$  by  $\langle N_{part} \rangle / 2$  as a function of  $\langle N_{part} \rangle$  at mid-rapidity ( $|y| < 0.1$ ) of  $\pi^+$ ,  $k^+$ ,  $p$  and  $\bar{p}$  for U+U collisions at  $\sqrt{s_{NN}}=193$  GeV. The red solid circles represent experimental data taken from the STAR Collaboration<sup>[23]</sup>. The black diamonds are the calculation using UrQMD model.

aspects will be investigated more thoroughly in future studies.

#### D. Particle ratios

Fig. 6 illustrates the ratios of  $\pi^-/\pi^+$ ,  $k^-/k^+$ , and  $\bar{p}/p$  as a function of  $\langle N_{part} \rangle$  at midrapidity ( $|y| < 0.1$ ) for U+U collisions at  $\sqrt{s_{NN}} = 193$  GeV. The black diamonds represent results from UrQMD calculations, while the red solid circles denote experimental data as reported in Ref. [23]. It is observed that the experimental findings align well within the margin of error. For both  $\pi$  and  $k$ , the yield ratios are nearly identical and remain approximately constant across different conditions. This indicates that positive and negative mesons are produced in pairs. In contrast, for the ratio of  $\bar{p}/p$ , there is a slight downward trend observed from peripheral to central collisions. This indicates that the more central

the collision, the stronger the blocking effect on protons. Considering that the UrQMD model does not explicitly include the quark-gluon plasma (QGP) phase transition, it may underestimate the corrective effect of the collective flow effect between partons in the central collision on the antiproton/proton yield ratio.

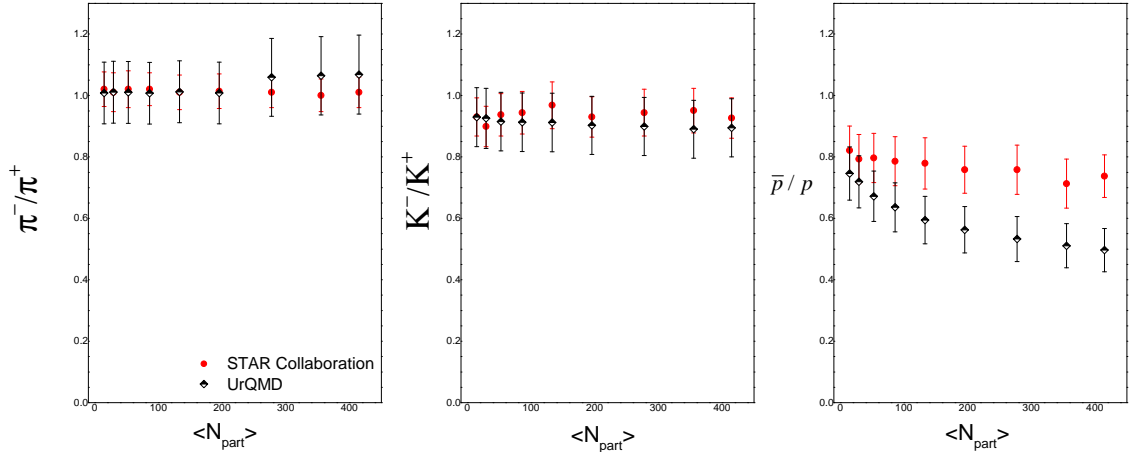


FIG. 6:  $\pi^-/\pi^+$ ,  $k^-/k^+$  and  $\bar{p}/p$  as a function of  $\langle N_{part} \rangle$  at mid-rapidity ( $|y| < 0.1$ ) for U+U collisions at  $\sqrt{s_{NN}}=193$  GeV. The experimental data of the STAR Collaboration <sup>[23]</sup> used in this analysis is shown as red solid circles. The black diamonds are the calculation using UrQMD model.

#### IV. SUMMARY AND OUTLOOK

In summary, within the centrality classes of 0–5%, 5–10%, 10–20%, 20–30%, 30–40%, 40–50%, 50–60%, 60–70%, and 70–80% in U+U collisions at  $\sqrt{s_{NN}} = 193$  GeV, we measured the transverse momentum spectra of  $\pi^\pm$ ,  $K^\pm$ , and  $p(\bar{p})$  in mid-rapidity ( $|y| < 0.1$ ). Additionally, other extracted observables from the transverse momentum spectra such as average transverse momentum ( $\langle p_T \rangle$ ), particle yields ( $dN/dy$ ), and particle ratios are presented as functions of collision centrality. We analyzed the experimental results from the STAR Collaboration <sup>[23]</sup> using the UrQMD model and found that the U+U collision process is subregional <sup>[37]</sup>, primarily due to the fact that uranium nuclei exhibit significant deformation. This non-spherical symmetry leads to variations in compression rates and lifetimes

of the central high-density material formed during collisions when U+U collides along different directions. The experimental data are well described by cascade mode for transverse momenta ( $p_T$ ) less than 1.2 GeV/c. However, for values greater than 1.2 GeV/c, discrepancies between calculations based on the SM-EoS model and experimental data increase as collision centrality decreases. Notably, as transverse momentum increases, theoretical predictions converge towards experimental results. It is important to note that since the UrQMD model does not incorporate a description of quark-gluon plasma nor adequately account for certain partons, this limitation contributes to observed differences between calculated outcomes and experimental observations. At RHIC energy levels, anti-baryon to baryon yield ratios suggest that pair production is a dominant mechanism underlying particle production processes. Next, we will explore strategies to enhance the model with the aim of accurately representing the experimental results.

### **Conflict of Interests**

The authors declare that there is no conflict of interests regarding the publication of this paper.

### **Acknowledgements**

We are grateful to the C3S2 computing center in Huzhou University for calculation support. This study used computational resources provided by Institute of Marine Drugs, Guangxi University of Chinese Medicine and the special Fund for Hundred Talents Program for Universities in Guangxi (Gui2019-71). The authors acknowledge the Beijing Super Cloud Computing Center (BSCC) for providing HPC resources that have contributed to the research results reported within this paper. URL: <http://www.blsc.cn/> This work was supported by the Fund for Less Developed Regions of the National Natural Science Foundation of China under Grant No.12365017, the Natural Science Foundation of Guangxi Zhuangzu Autonomous Region of China under Grant No. 2021GXNSFAA196052, the Introduction of Doctoral Starting Funds of Scientific Research of Guangxi University of Chinese Medicine under Grant No.2018BS024, and the Open Project of Guangxi Key Laboratory of Nuclear Physics and Nuclear Technology, No. NLK2020-03.

- 
- [1] C. Alt *et al.* [NA49 Collaboration], “Energy dependence of  $\Lambda$  and  $\Xi$  production in central Pb+Pb collisions at 20A, 30A, 40A, 80A, and 158A GeV measured at the CERN Super Proton Synchrotron,” *Physical Review C*, vol. 78, no. 3, Article ID 034918, 2008.
  - [2] J. X. Sun, F. H. Liu and E. Q. Wang, “Pseudorapidity Distributions of Charged Particles and Contributions of Leading Nucleons in Cu-Cu Collisions at High Energies,” *Chinese Physics Letters*, vol. 27, no. 3, Article ID 032503, 2010.
  - [3] E. Q. Wang, F. H. Liu, M. A. Rahim, S. Fakhraddin, J. X. Sun, “Singly and Doubly Charged Projectile Fragments in Nucleus-Emulsion Collisions at Dubna Energy in the Framework of the Multi-Source Model,” *Chinese Physics Letters*, vol. 28, no. 8, Article ID 082501, 2011.
  - [4] B. C. Li, and M. Huang, “Strongly coupled matter near phase transition,” *Journal of Physics G-Nuclear and Particle Physics*, vol. 36, Article ID 064062, 2009.
  - [5] F. H. Liu, “Anisotropic emission of charged mesons and structure characteristic of emission source in heavy ion collisions at 1–2A GeV,” *Chinese Physics B*, vol. 17, no. 3, pp. 883-895, 2008.
  - [6] M. I. Abdulhamid, *et al.* [STAR Collaboration], “Measurement of electrons from open heavy-flavor hadron decays in Au+Au collisions at  $\sqrt{s_{NN}} = 200$  GeV with the STAR detector,” *J. High Energ. Phys.*, vol. 2023, Article number 176, 2023.
  - [7] J. Adam, *et al.* [STAR Collaboration], “Beam-energy dependence of the directed flow of deuterons in Au+Au collisions,” *Phys. Rev. C*, vol. 102, Article ID 044906, 2020.
  - [8] R. Arsenescu *et al.* [NA52 Collaboration], “An investigation of the antinuclei and nuclei production mechanism in Pb + Pb collisions at 158 A GeV,” *New Journal of Physics*, vol. 5, pp. 150, 2003.
  - [9] Q. F. Li, Y. J. Wang, X. B. Wang and C. W. Shen, “Helium-3 production from Pb+Pb collisions at SPS energies with the UrQMD model and the traditional coalescence afterburner,” *Science China: Physics, Mechanics and Astronomy*, vol. 59, no. 3, Article ID 632002, 2016.
  - [10] H. L. Lao, H. R. Wei, F. H. Liu and Roy A. Lacey, “An evidence of mass-dependent differential kinetic freeze-out scenario observed in Pb-Pb collisions at 2.76 TeV,” *European Physical Journal A*, vol. 52, Article ID 203, 2016.
  - [11] S. Mrowczynski, P. Slon, “Hadron-Deuteron Correlations and Production of Light Nuclei in

- Relativistic Heavy-Ion Collisions,” *Acta Physica Polonica B*, vol. 51, Article ID 1739, 2020.
- [12] St. Mrowczynski, “Production of Light Nuclei in the Thermal and Coalescence Models,” *Acta Physica Polonica B*, vol. 48, pp. 707, 2017.
- [13] St. Mrowczynski, “ $^4\text{He}$  versus  $^4\text{Li}$  and production of light nuclei in relativistic heavy-ion collisions,” *Modern Physics Letters A*, vol. 33, Article ID 1850142, 2018.
- [14] P. Liu, J. H. Chen, Y. G. Ma and S. Zhang, “Production of light nuclei and hypernuclei at High Intensity Accelerator Facility energy region,” *Nuclear Science and Techniques*, vol. 28, Article ID 55, 2017.
- [15] F. X. Liu, G. Chen, Z. L. Zhe, D. M. Zhou and Y. L. Xie, “Light (anti)nuclei production in Cu+Cu collisions at  $\sqrt{s_{NN}}=200$  GeV,” *European Physical Journal A*, vol. 55, Article ID 160, 2019.
- [16] Y. Yuan, Q. F. Li, Z. X. Li, and F. H. Liu, “Transport model study of nuclear stopping in heavy-ion collisions over the energy range from 0.09A to 160A GeV,” *Physical Review C*, vol. 81, Article ID 034913, 2010.
- [17] Y. Yuan, “Study of Production of (Anti-)deuteron Observed in Au+Au Collisions at  $\sqrt{s_{NN}}=14.5, 62.4$ , and 200 GeV,” *Advances in High Energy Physics*, vol. 2021, Article ID 9305605, 2021.
- [18] P. C. Li, Y. J. Wang, Q. F. Li, H. F. Zhang, “Assessing the in-medium effects on nucleon-nucleon elastic cross section with collective flows and nuclear stopping,” *Physics Letters B*, vol. 828, Article ID 137019, 2022.
- [19] Y. Yuan, Z. Q. Huang, X. F. Zhang, X. Z. Wei, “Transport model study of transverse momentum distributions of (anti-)deuterons production in Au+Au collisions at  $\sqrt{s_{NN}}=14.5, 62.4$ , and 200 GeV,” *Frontiers in Physics*, vol. 10, Article ID 971407, 2022.
- [20] B. C. Li, Y. Y. Fu, L. L. Wang, F. H. Liu, “Dependence of elliptic flows on transverse momentum and number of participants in AuAu collisions at 200 GeV,” *Journal of Physics G-Nuclear and Particle Physics*, vol. 40, Article ID 025104, 2013.
- [21] Y. H. Chen, F. H. Liu and Edward K. Sarkisyan-Grinbaum, “Event patterns from negative pion spectra in proton-proton and nucleus-nucleus collisions at SPS,” *Chinese Physics C*, vol. 42, no. 10, Article ID 104102, 2018.
- [22] M. S. Abdallah, *et al.* [STAR Collaboration], “Azimuthal anisotropy measurement of (multi)strange hadrons in Au+Au collisions at  $\sqrt{s_{NN}}=54.4$  GeV,” *Physical Review C*, vol.

107, Article ID 024912, 2023.

- [23] M. S. Abdallah, *et al.* [STAR Collaboration], “Pion, kaon, and (anti) proton production in U+U collisions at  $\sqrt{s_{NN}}=193$  GeV measured with the STAR detector” *Physical Review C*, vol. 107, Article ID 024901, 2023.
- [24] H. Petersen, M. Bleicher, S. A. Bass and H. Stocker, “UrQMD-2.3 - Changes and Comparisons,” <http://arxiv.org/abs/0805.0567>.
- [25] B. Andersson, G. Gustafson and B. Nilsson-Almqvist, “A Model For Low P(T) Hadronic Reactions, With Generalizations To Hadron-Nucleus And Nucleus-Nucleus Collisions,” *Nuclear Physics B*, vol. 281, no. 1-2, pp. 289-309, 1987.
- [26] B. Nilsson-Almqvist and E. Stenlund, “Interactions Between Hadrons And Nuclei: The Lund Monte Carlo, Fritiof Version 1.6,” *Computer Physics Communications*, vol. 43, no. 3, pp. 387-397, 1987.
- [27] T. Sjostrand, “High-energy physics event generation with PYTHIA 5.7 and JETSET 7.4,” *Computer Physics Communications*, vol. 82, no. 1, pp. 74-89, 1994.
- [28] S. A. Bass, M. Belkacem, M. Bleicher, M. Brandstetter, L. Bravina, C. Ernst, L. Gerland, M. Hofmann, S. Hofmann, J. Konopka, G. Mao, L. Neise, S. Soff, C. Spieles, H. Weber, L. A. Winckelmann, H. Stocker and W. Greiner, “Microscopic models for ultrarelativistic heavy ion collisions,” *Progress in Particle and Nuclear Physics*, vol. 41, pp. 255-369, 1998.
- [29] H. Petersen, Q. F. Li, X. L. Zhu and M. Bleicher, “Directed and elliptic flow in heavy-ion collisions from  $E_{beam} = 90$  MeV/nucleon to  $E_{c.m.} = 200$  GeV/nucleon,” *Physical Review C*, vol. 74, Article ID 064908, 2006.
- [30] Gao Z P, Wang Y J, Li Q F, et al., “Application of machine learning to study the effects of quadrupole deformation on the nucleus in heavy-ion collisions at intermediate energies (in Chinese),” *Sci Sin-Phys Mech Astron*, vol. 52, Article ID 252010, 2022.
- [31] M. I. Abdulhamid, *et al.* [STAR Collaboration], “Imaging shapes of atomic nuclei in high-energy nuclear collisions” *Nature*, vol. 635, 67-72, 2024.
- [32] Kai Zhao, Zhuxia Li, Xizhen Wu and Yingxun Zhang, “Production probability of superheavy fragments at various initial deformations and orientations in the  $^{238}\text{U}+^{238}\text{U}$  reaction,” *Physical Review C*, vol. 88, Article ID 044605, 2013.
- [33] M. Bleicher, E. Zabrodin, C. Spieles, S. A. Bass, C. Ernst, S. Soff, L. Bravina, M. Belkacem, H. Weber, H. Stocker and W. Greiner, “Relativistic hadron hadron collisions in the ultra-



- relativistic quantum molecular dynamics model,” *Journal of Physics G: Nuclear and Particle Physics*, vol. 25, no. 9, pp. 1859-1896, 1999.
- [34] S. A. Bass, C. Hartnack, H. Stocker and W. Greiner, “Azimuthal correlations of pions in relativistic heavy ion collisions at 1GeV/nucleon,” *Physical Review C*, vol. 51, no. 6, pp. 3343-3356, 1995.
- [35] Q. F. Li, Z. X. Li, S. Soff, M. Bleicher and H. Stoecker, “Probing the equation of state with pions,” *Journal of Physics G: Nuclear and Particle Physics*, vol. 32, no. 2, pp. 151-164, 2006.
- [36] Q. F. Li and M. Bleicher, “A model comparison of resonance lifetime modifications, a soft equation of state and non-Gaussian effects on  $\pi - \pi$  correlations at FAIR/AGS energies,” *Journal of Physics G: Nuclear and Particle Physics*, vol. 36, no. 1, Article ID 015111, 2009.
- [37] K. J. Wu, X. F. Luo and F. Liu, “Simulation for Elliptic Flow of UU Collisions at CSR Energy Region in Lanzhou,” *Chinese Physics C*, vol. 31, no. 7, pp. 617-620, 2007.